frontiers | Frontiers in Catalysis

TYPE Original Research
PUBLISHED 01 November 2022
DOI 10.3389/fctls.2022.1006564



OPEN ACCESS

EDITED BY
Suresh Sagadevan,
University of Malaya, Malaysia

REVIEWED BY
Thillai Sivakumar Natarajan,
Central Leather Research Institute (CSIR), India
Buzuayehu Abebe,
Adama Science and Technology University, Ethiopia

*CORRESPONDENCE
Andres Fullana,
andres.fullana@ua.es

SPECIALTY SECTION
This article was submitted to Photocatalysis, a section of the journal Frontiers in Catalysis

RECEIVED 29 July 2022
ACCEPTED 17 October 2022
PUBLISHED 01 November 2022

CITATION
Flores-Oña D and Fullana A (2022), High efficient solar photocatalytic carbon nanoparticles.
*Front. Catal.* 2:1006564.
doi: 10.3389/fctls.2022.1006564



# High efficient solar photocatalytic carbon nanoparticles

Diego Flores-Oña[1] and Andres Fullana[2]*

[1]Chemical Engineering Faculty, Universidad Central Del Ecuador, Quito, Ecuador, [2]Department of Chemical Engineering, Universidad de Alicante, Alicante, Spain

In the present study, the photocatalytic activity of carbon nanoparticles (CNPs) in the degradation of methylene blue (MB) using sunlight was analyzed. The CNPs were synthesized by solvent-assisted hydrothermal carbonization (HTC) and were characterized by various spectroscopic techniques: TEM and SEM microscopy, UV-Vis, FTIR, Fluorescence, and XPS. By changing the conditions of the HTC process, the surface chemistry of CNPs was functionalized, thus a great quantity of oxygenated functional groups was generated, which eventually influenced the photocatalytic process. Next, tests were carried out with different types of nanoparticles, varying the concentration of the dye and the type of light used in the irradiation. As a result of this, more than 93% of MB degradation was achieved in 20 min of irradiation using sunlight. This result is promising since it has not been achieved by other nanomaterial. This research can be a potential starting point for the development of new solar photocatalysts.

KEYWORDS

**photocatalysts, carbon nanoparticles, sunlight, hydroxyl radicals, methyl blue**

## 1 Introduction

Methylene blue (MB) is a chemical compound used in numerous industrial applications. This colorant alters the pH, turbidity, COD, suspended solids, and conductivity of wastewater; consequently, there is a need to treat colored effluents before discharging them into the environment. Currently, there are several treatment processes that include treatments such as physical, chemical, and biological (Siddique et al., 2017); however, recent research has focused on the development of clean technologies based on advanced oxidation processes, such as ozonation, ultraviolet radiation, fenton processes, photo-fenton processes, electrochemical oxidation, and photocatalysis (Miklos et al., 2018). Photocatalytic degradation of colorants has had a great impact in recent decades because it is a low-cost and environmentally-friendly

**Abbreviations:** HTC, hydrothermal carbonization; CNP, carbon nanoparticles; CNP-W; carbon nanoparticles synthesized in standard hydrothermal carbonization; CNP-SA, carbon nanoparticles synthesized in solvent assisted hydrothermal carbonization; MB, methylene blue.

method since it can reach the mineralization of the dye (Kumar and Pandey, 2017). Photocatalytic processes occur when a photocatalyst is irradiated with UV-Vis energy. The energy of the photon that is greater than that of the photocatalyst band gap's, will promote electrons from the valence band to the conduction band and produce a hole-electron pair. The electrons and holes generate hydroxyl and superoxide radicals, which can decompose organic pollutants in a redox process (Wang et al., 2017).

Semiconductors have been one of the first photocatalysts studied in pollutant degradation processes. The most representative semiconductor is titanium dioxide, $TiO_2$, which has exceptional chemical stability, low toxicity, low cost, easy accessibility, and high photocatalytic activity (Chen et al., 2020). However, $TiO_2$ has a major weakness, its band gap has a value of around 3.22 eV, which implies that only ultraviolet light can excite the electrons to produce the hole-electron pair (Makuła et al., 2018), this results in a more expensive process since sunlight cannot be harnessed.

Recent research focuses on the development of photocatalysts that are activated by visible light to increase the efficient use of sunlight. Among these materials are semiconductor nanomaterials, nanocrystals (Buzuayehu and Ananda, 2022) and carbon nanomaterials, which include carbon nanoparticles (CNP) and carbon quantum dots (CQD). These nanomaterials are a new form of nanostructured carbon with excellent photophysical properties, especially photoluminescence at specific wavelengths. In the study carried out by (Zhu et al., 2015) carbon nanodots with excellent photocatalyst properties to drive hydrogen generation as a source of renewable energy. On the other hand, the photoluminescent properties of carbon dots have been tested as sensors and bioimaging, obtaining nanomaterials potentially be used in anti-counterfeit applications and detecting $Fe^{3+}$ in biosystems (Zhu et al., 2013). In addition, in the study carried out by (Mazrad et al., 2018), fluorescent carbon nanoparticles are effortless to functionalize for intracellular detection.

Carbonaceous nanomaterials are prepared by chemical oxidation, graphite oxidation, electrochemical oxidation, laser ablation, electrochemical exfoliation, microwave pyrolysis of saccharides, or thermal oxidation of residual biomass sources (Lee et al., 2019). However, these processes usually involve expensive equipment, harsh synthesis conditions, or require post-treatment processes. On the other hand, a cost-effective and environmentally-friendly alternative for obtaining CNP, is hydrothermal carbonization (HTC), a process that is carried out under relatively low-temperature conditions and with self-generated pressures and could potentially convert biomass into carbonaceous materials with high photocatalytic power (Román et al., 2018).

One of the variables of the HTC process is the type of solvent used, which will influence the chemical composition and optical properties of the carbon nanoparticles obtained. In a previous study (Flores-Oña and Fullana, 2020), CNPs were synthesized using two processes: the first one is a standard HTC process, where water is used as a solvent; while the second was a solvent-assisted HTC process, where a mixture of water with butyl acetate was used. This variation in the process changed the CNPs' surface chemistry, they ended up with a high amount of surface oxygenated groups, which might influence their ability to generate electron-hole pairs, and consequently hydroxyl radicals. The objective of this research is to study the behavior of these CNPs in the photocatalytic process for the degradation of MB; with visible light obtained by lamps inside a photoreactor, as well as, with sunlight, thus offering a sustainable possibility for the design and use of carbonaceous materials for the photodegradation of dyes.

# 2 Materials and methods

## 2.1 Chemicals

D-(+)-Glucose (purity 99,5%), butyl acetate GR, methanol GR, methylene blue (purity >97%) were obtained from commercial sources.

## 2.2 Synthesis

### 2.2.1 Carbon nanoparticles by standard hydrothermal carbonization r

Dissolve 10 g of glucose in 400 ml of distilled water. The solution is placed in a stainless-steel reactor of 500 ml capacity. It is heated up to 200°C during 1 h, then the reactor is cooled down, and the hydrochar is separated by filtration, using a membrane filter of 0.45 μm. Then, the liquid is ultra-centrifuged for a time of 15 min at 20,000 rpm. After that, the water is evaporated in a rotary evaporator, and finally, the CNP are dried in a lab oven for 2 h.

### 2.2.2 Carbon nanoparticles by solvent assisted hydrothermal carbonization

Dissolve 10 g of glucose in 300 ml of distilled water, add 100 ml of butyl acetate and place the blend into a stainless-steel reactor of 500 ml capacity. It is heated up to 200°C during 1 h, then the reactor is cooled down, and the hydrochar is separated by filtration, using a membrane filter of 0.45 μm. The blend is settled down for 10 min. Then, the phases are separated, and the organic phase is ultra-centrifuged for a time of 15 min at 20,000 rpm. After that, the organic solvent is evaporated in a rotary evaporator, and finally, the CNP are dried in a lab oven for 2 h.

### 2.2.3 Photocatalytic degradation

Place 100 mg of CNP and 1 ml of solvent in a reactor and stir to disperse the carbon nanoparticles. Add 100 ml of a methylene

blue (MB) solution. The reactor is irradiated with visible light, maintaining constant agitation. After a certain time, the solution is passed through a 0.45 μm filter and the absorbance of the MB is measured by UV-Vis spectrophotometry at a wavelength of 665 nm. The concentrations of MB are calculated by a calibration curve prepared with a MB standard solution. The procedure is repeated with the following modifications: type of solvent to disperse the nanoparticles: water, butyl acetate, and methanol; MB concentration: 30 ppm and 60 ppm; irradiation time: from 1 to 80 min; and type of visible light: visible light obtained in a photoreactor and sunlight. The photoreactor uses LZC-Vis type fluorescent lamps, which emit 92% energy in the range of 400 nm–700nm, 3% UVA light, <1% UVB light, and <1% UVC light.

## 2.3 Characterization methods

CNP-W and CNP-SA were analyzed to study the physical, chemical, and optical properties using Electron Microscopy, Fourier Transform Infrared (FTIR) spectroscopy, ultraviolet-visible (UV-Vis) spectroscopy, fhotoluminescence (PL) spectroscopy, and X-Ray photoelectron spectroscopy (XPS). FESEM images were obtained by using a Carl Zeiss microscope. TEM images were taken using a TEM-200 microscope operating at 200 kV. The functional groups in the infrared spectra were analyzed using a Perkin Elmer Spectrum Two FT-IR Spectrometer. Absorption spectra and the residual concentration of MB was performed by using a Cary 60 UV–Vis spectrophotometer (Agilent). Emission spectra for PL map were measured with BioTek Synergy H1 spectrometer. Photoluminescence Quantum Yield (PL QY) were determined with an integrating sphere equipped on an Edimburgh Instruments FS5 spectrofluorimeter. XPS spectra for O1s and C1s were taken in a K-Alpha Spectrometer.

# 3 Results and discussion

The carbon nanoparticles' surface chemistry is important in the generation of hydroxyl radicals for the photocatalysis process, in this study two types of nanoparticles were tested in the photodegradation on MB: nanoparticles obtained from a standard HTC process in an aqueous medium (CNP-W); and nanoparticles synthesized from a solvent-assisted HTC process (CNP-SA), which are generated in a mixture of water with butyl acetate.

## 3.1 Characterization

Carbon nanoparticles synthesized in aqueous medium (CNP-W), as well as, in the solvent-assisted process (CNP-SA) have a spherical shape with a broad size dispersion. Figure 1 shows the TEM and FESEM images obtained for both samples. In standard HTC, the number of nanoparticles that are formed is small, due to the short synthesis time, which makes it difficult to find them in the microscope grids (Figures 1A,B). On the other hand, the amount of nanoparticles in the modified method is greater than in the standard process, which can be observed in Figures 1C,D; however, the high degree of size dispersion is kept, ranging from 80 nm to 275 nm. Therefore, by modifying the synthesis method, a greater formation of nanoparticles is achieved, but with highly dispersed sizes.

The chemical structure of the CNP synthesized in the HTC process was analyzed by FT-IR spectroscopy. Figure 2A shows the infrared spectra of CNP-W and CNP-SA. The band at 3370 $cm^{-1}$ corresponds to the hydroxyl group (O-H), while the band at 2995$cm^{-1}$ to aliphatic groups (C-H). On the other hand, the band at 1650$cm^{-1}$ is attributed to the carbonyl group (C = O), while the band at 1395$cm^{-1}$ corresponds to the aromatic groups (C=C). The band at 1046$cm^{-1}$ is from the ether and ester groups (C-O-C/C-O); and finally, the band at 844$cm^{-1}$ corresponds to aromatics (C-H).

In both: CNP-W and CNP-SA, the bands corresponding to the hydroxyl group (3370$cm^{-1}$) and the aliphatic group (2995$cm^{-1}$) have the same intensity. Thus, the amount of these functional groups in both nanoparticles are the same, therefore, the dehydration process that glucose had in the HTC reactor has an equal intensity for both type of nanoparticles. Moreover, the carbonyl group (1650$cm^{-1}$) and the aromatic groups (1395$cm^{-1}$) present in CNP-SA, have a higher intensity than CNP-W's, which means that the solvent-assisted HTC produce a greater formation of aromatic structures and specifically of oxygenated groups (C=O/C-O), functional groups involved in the process for the generation of electron-hole pairs.

The optical properties of carbon nanoparticles are fundamental in photocatalytic processes, Figure 2B shows the absorption spectrum of CNP-W and CNP-SA. Both nanoparticles have a peak with an absorption maximum located in the ultraviolet region, at 280 nm. This peak corresponds to $\pi$-$\pi^*$ transitions of carbons with double bonds (C=C), which are in aromatic compounds, dominant in CNP. The spectra have a tail that extends along the visible region, corresponding to the other functional groups on the surface of CNP, such as carboxyl and carbonyl (C=O), which generate peaks due to n-$\pi^*$ transitions. The absorption spectra of the synthesized CNPs show a small peak at 327 nm, with a stronger intensity in the CNP-SA than in the CNP-W, this behavior was expected due to the greater number of oxygenated groups (C=O) from nanoparticles synthesized in the solvent-assisted HTC process.

Figure 3 shows the high-resolution XPS spectra for CNP-W and CNP-SA. In the O1s spectrum, two peaks are observed, one at 532.1 eV and the second at 533.3 eV corresponding to the C=O and C-O bonds. Likewise, the C1s spectrum shows three peaks at

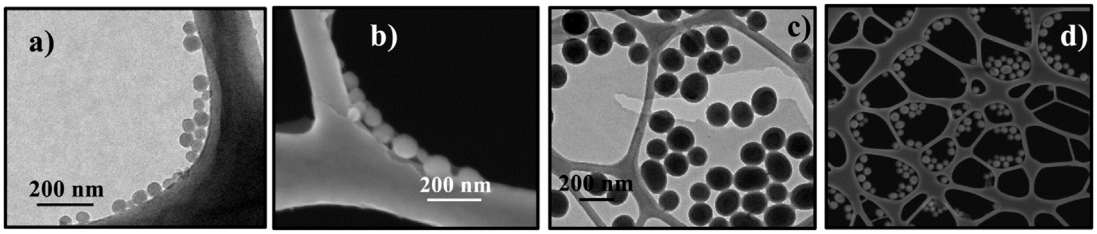


FIGURE 1
**(A)** TEM image for CNP-W, **(B)** FESEM image for CNP-W, **(C)** TEM image for CNP-SA, **(D)** FESEM image for CNP-SA.

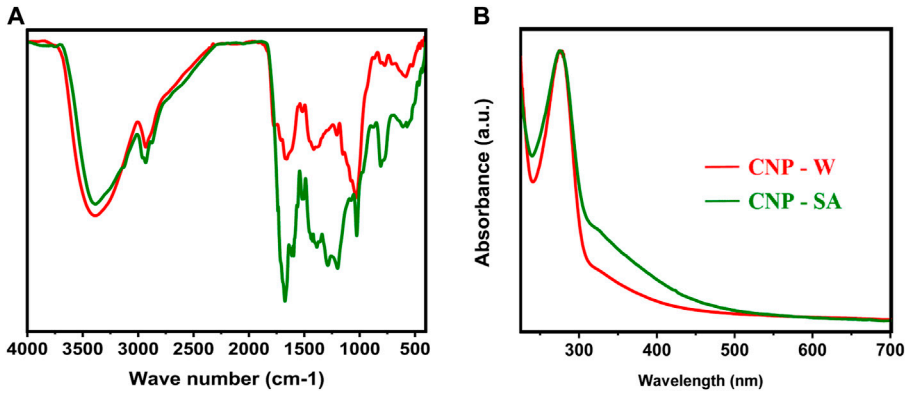


FIGURE 2
**(A)** IR spectrum of CNP-W and CNP-SA, **(B)** Absorption spectrum of CNP-W and CNP-SA.

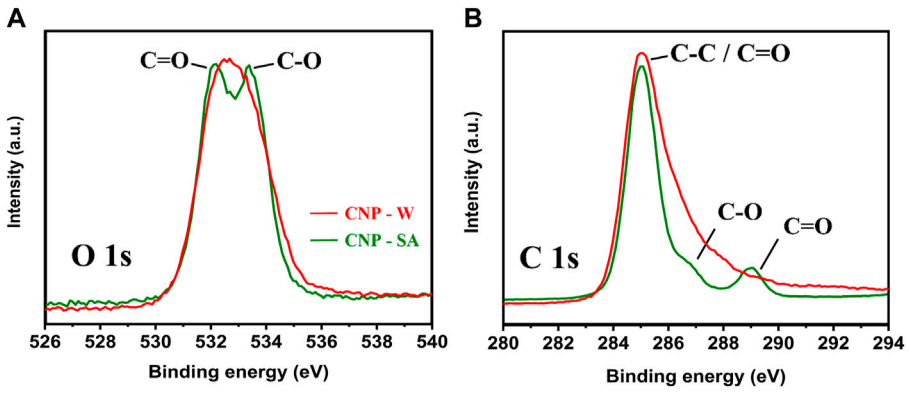


FIGURE 3
High-resolution XPS spectrum of CNP **(A)** O1s, **(B)** C1s.

285.0, 286.8, and 288.0, which correspond to the C-C/C=C, C-O, and C =O bonds. It is clearly visible that, for the CNP-SA there is a better definition of the peaks corresponding to the oxygenated groups in both spectra: O1s and C1s. This means that CNP-SA present a greater number of oxygenated groups, C=O/CO, as seen in FT-IR spectra.

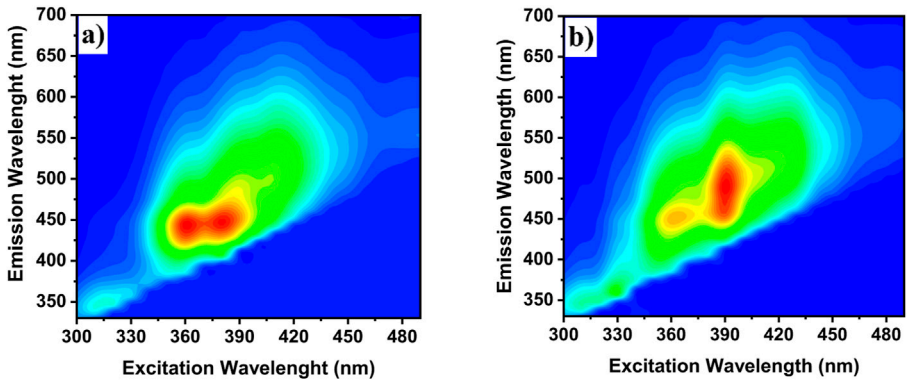


FIGURE 4
PL map for carbon nanoparticles **(A)** CNP-W, **(B)** CNP-SA.

A carbon nanoparticle that receives energy with a specific wavelength, produces a phenomenon known as absorption, where an electron takes the energy and goes from a fundamental state to an excited state, generating an electron-hole pair. Recombination of the photogenerated electron-hole pair contributes to luminescence and depends on the chemical composition of the carbon nanoparticles. In our case, CNPs exhibit photoluminescence (PL) that is dependent on excitation, a phenomenon typical of fluorescent carbonaceous materials (Wang et al., 2014). Figure 4 shows PL maps for CNP-W and CNP-SA, obtained from the compilation of emission spectra, taken at different excitation wavelengths, from 300 nm to 490 nm with 10 nm intervals. The PL maps show a greater fluorescence area for CNP-SA compared to CNP-W. Hence, CNP-SA can be excited in a wider wavelength range, and they will be able to take the energy visible from the Sun. On the other hand, in CNP-W only a zone with maximum fluorescence intensity at 450 nm corresponding to the blue color is observed; while for CNP-SA, an additional fluorescence zone is observed, that extends up to 525 nm. Consequently, the CNP-SA, fluoresce in a wider range that moves from the blue color to the green color.

In the research (Hu et al., 2013), the optical behavior of CNP was attributed to different surface defects. Hu demonstrated through experiments and theoretical analysis that the luminescence centers come from the mixture of sp2 and sp3 bonds; and that surface groups such as hydroxyl, carbonyl, carboxyl, and epoxy trap the electron in the radiative recombination process, avoiding the emission of light and obtaining small fluorescence quantum yield (PL QY). Also, in the study (Sun et al., 2014), CNPs that form an aromatic carbonaceous structure with carbonyl and carboxyl surface functional groups, tend to form green luminescence centers with a small PL QY [Zhuo et al., 2012; Yang et al., 2015), a phenomenon that is evidenced in CNP-SA, which have a PL QY of 1.59% and a luminescence that tends to a green color. Therefore, this phenomenon is happening in the CNP-SA, the intensity of PL indicates very small recombination of the electron-hole. In other words, the electron in the excited state has not returned to the fundamental state, and the electron-hole could be used for oxidation-reduction processes (Wang et al., 2015).

## 3.2 Photocatalytic degradation

For the determination of the photocatalytic activity of CNPs, photodegradation of a solution of methylene blue (MB) was analyzed. The photodegradation of MB is evidenced by the decrease in absorbance measured in a spectrophotometer at a wavelength of 655 nm. In addition, photodegradation can be observed by changing the color of the MB solution, the initial solution is blue and as the irradiation time increases it gets colorless.

Due to the surface chemistry of CNP, one of the aspects to consider in photocatalysis is the dispersion of the nanoparticles. A good dispersion ensures that the active centers are free for the light to get hydroxyl radicals and the oxidation reaction takes place. CNP-W disperse easily in water; while CNP-SA, being less polar, have difficulty dispersing in an aqueous solution and do better in organic solvents. As a result of this, the photocatalysis was carried out testing three solvents to disperse the nanoparticles: water, butyl acetate, and methanol, the results are shown in Figure 5. The energy source for the assays was visible light obtained by lamps inside a photoreactor.

Figure 5A shows the photocatalytic reaction of CNP-W dispersed in the three solvents: water, butyl acetate, and methanol, with a percentage of MB degradation of 70.3%, 68.9%, and 64.5% respectively. After 20 min of irradiation, photocatalysis has stopped, the active centers of the nanoparticles no longer generate hydroxyl radicals, and the

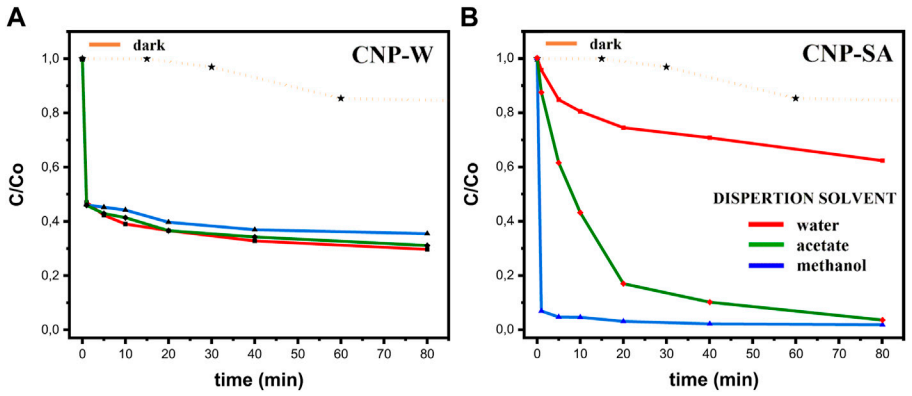


FIGURE 5
MB concentration as a function of irradiation time with visible light, **(A)** CNP-W dispersed in various solvents, **(B)** CNP-SA dispersed in various solvents.

concentration of MB remains almost constant. This phenomenon has possibly been observed due to the fact that solvent does not allow a complete dispersion of the particles despite of the used solvent. The dispersion of CNP-W in different solvents does not affect their photocatalytic activity. On the contrary, for CNP-SA, the solvent does have a positive effect. When dispersing the CNP-SA in water, the degradation of the MB is small, reaching only 37.8%; but, with less polar solvents such as butyl acetate and methanol, the degradation is effective, with 80 min of irradiation there is a degradation of the MB of 96.5% and 98.2%, respectively.

The results shown in Figure 5 determine that CNP-SA are better photocatalysts than CNP-W. When the CNP-SA are used, complete degradation of the MB is achieved, for this reason, CNP-W are discarded, and the following tests are performed only with CNP-SA. On the other hand, the results obtained from CNP-SA that were dispersed in butyl acetate and methanol are more effective than that of the results obtained from CNP-SA that were dispersed in water; this is due the nanoparticles having non-polar chemistry and being better dispersed in solvents with low polarity than in solvents with a high polarity such as water. By improving the dispersion, there are a greater number of active sites of the photocatalyst for the degradation of MB and thus the process is more efficient. We decided to work only with methanol, because it presents the best results in terms of the degradation percentage, in just 1 min of irradiation, the MB degrades 93.2%.

To verify the degradation of MB is due to a photocatalytic process and not to an adsorption process, the following analysis was carried out. The CNP-SA were dispersed in methanol and irradiation with visible light, but the reactor was completely covered from light. In Figures 5, 6, the broken line, called dark, represents the performed experiment. The concentration of MB remains almost constant, only a small decrease in MB

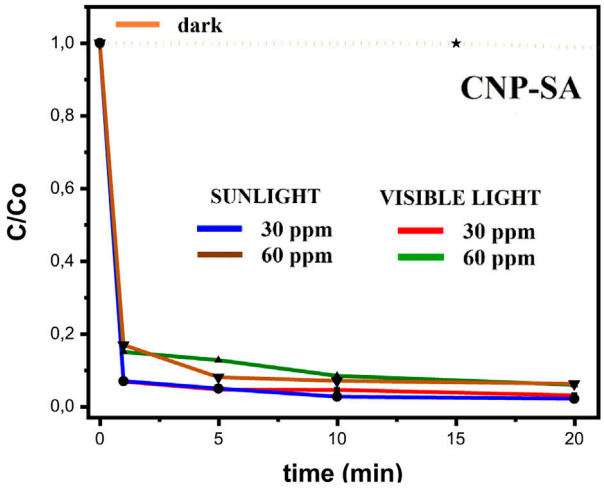


FIGURE 6
MB concentration as a function of irradiation time with visible light and sunlight with different concentrations of the dye using CNP-SA.

concentration is registered. With this test, we determined that the process that governs the degradation of MB is photocatalysis because, in 1 minute, the dye degrades 93.2%; and in adsorption, after 15 min, 0.1% is adsorbed.

The reaction mechanism for the photodegradation of MB has been studied by several authors (Subagyo et al., 2020; Deshmukh et al., 2020). They mention that visible light forms the electron-hole pair; the holes react with water to produce hydroxyl radicals (OH•) and the electrons react with dissolved oxygen on the surface of nanoparticles to form superoxide radicals (O2•-), which through a secondary chemical reaction can also produce hydroxyl radicals. Therefore, the oxidative capacity of

TABLE 1 Comparison of results obtained for the degradation of MB with different photocatalysts.

| Catalyst | Degradation (%) | Light source | Irradiation time (min) | Catalyst preparation | Catalyst mass (g/L) | MB initial concentration (ppm) | Ref |
|---|---|---|---|---|---|---|---|
| CNP | 93.8 | Sunlight | 20 | HTC | 1.0 | 60 | This study |
| CNP | 94.0 | Visible | 20 | HTC | 1.0 | 60 | This study |
| CNP | 97.9 | Sunlight | 20 | HTC | 1.0 | 30 | This study |
| CNP | 97.0 | Visible | 20 | HTC | 1.0 | 30 | This study |
| Silicio-CNP | 98.8 | Visible | 75 | Thermal | 0.5 | 10 | Wang et al. (2021) |
| Nitrogen-Carbon Quantum Dots | 97.0 | Sunlight | 180 | Hydrothermal | 0.1 | 10 | Ng et al. (2020) |
| Graphene Oxide-TiO2 | 91.3 | Sunlight | 30 | Sonochemical | 2.0 | 20 | Bhanvase et al. (2019) |
| Graphene Oxide—ZnO | 80.0 | Visible | 90 | HTC | 0.5 | 10 | Ranjith et al. (2017) |
| Magnetic C dots | 83,0 | Visible | 30 | Solvothermal | 1.0 | 120 | Kusumawati et al. (2019) |
| Graphene nanoplatelets -ZnO | 87.0 | UV-Visible | 60 | Solvothermal | 1.0 | 10 | Mahmud et al. (2020) |
| Activated carbon oxide - metal | 91.0 | UV | 60 | Physico-chemical | 0.1 | 100 | Murugesan et al. (2021) |

a photocatalyst will depend on the number of electron-hole pairs formed. At this point, the chemical structure of the carbon nanoparticle plays a fundamental role, to avoid the recombination of the electron-hole pair. In the studies by Hu (Hu et al., 2013), the photocatalytic process for photocatalysts doped with carbon quantum dots (CQD) in the degradation of MB was analyzed, and it was determined that the surface groups could create photogenerated charge traps. When the surface of the CQD is composed of carbonyl or carboxyl groups, there is a greater photocatalytic activity. On the contrary, when the surface of the CQD is made up of OH groups, a decrease in the photocatalytic process is induced. Hu deduces that the surface groups C=O and COOH create a large electric field near the surface of the CQD, which he calls *higher upward band bending*. This electric field separates the electron-hole pairs, reducing recombination and promoting the transport of the hole to the surface, in this way, the photocatalytic activity is improved. On the other hand, the surface -OH groups create a smaller electric field, or *lower upward band bending*, decreasing the separation of the electron-hole pair, facilitating their recombination. This could be the reason why CNP-SA exhibit more effective photocatalytic activity than CNP-W, due to CNP-SA having more carbonyl groups on its surface, thus making the electron-hole pair recombination small, eventually increasing the oxidative capacity of the photocatalyst.

For the next photocatalytic tests, the CNP-SA are dispersed in methanol, and two modifications are made to the process: the first one is to increase the molecules of MB to analyze the effect of the concentration of the dye, and the second one is to use sunlight instead of visible light, to determine whether the photodegradation can be carried out with energy from the Sun.

Figure 6 and Table 1 show a comparison of the MB photodegradation process using CNP-SA dispersed in methanol and irradiated with visible light and sunlight. In either case, an almost complete degradation of the MB is achieved; thus, sunlight can be used for the photocatalytic process. In the same way, by increasing the concentration of MB from 30 ppm to 60 ppm, high percentages of degradation are obtained regardless of the type of light.

Table 1 shows some studies that use nanoparticles for the photodegradation of MB, a comparison is made with an emphasis on the synthesis parameters of the nanoparticles and the conditions for the photocatalysis tests.

The study by Li et al. (2021) reaches a degradation percentage of 98.8%, but the synthesis time of the nanoparticles takes more than 6 h and requires a greater number of reagents; furthermore, the initial concentration of MB is much lower than that used in this research. On the other hand, Rani et al. (2021), achieved a MB degradation of 97.0%, but with an irradiation time of 180 min; moreover, to produce carbon quantum dots, three processes are required: pyrolysis, polymerization, and oxidation. In another way (Bhanvase et al., 2019), achieved a degradation of 91.3%, but with greater amount of the catalyst, and in a larger time. The other studies shown in table 1 do not get a considerable degradation percentage or use ultraviolet light as a source of irradiation. Therefore, to the best of our knowledge, none nanomaterial can achieve the results obtained with CNP-SA, using sunlight as the irradiation source.

## 4 Conclusion

Solar-activated photocatalysts have been successfully synthesized using a simple, short-time HTC method that does not require post-treatment. The superficial functional groups prevent the recombination of the electron-hole pair, increasing the oxidative capacity of CNP-SA. In the best conditions, the photodegradation of MB exceeds 93%, with just 20 min of exposure to sunlight. In this way, CNP-SA have superior photocatalytic properties with solar energy, making them a promising nanomaterial and a starting point for using in other redox processes.

## Data availability statement

The raw data supporting the conclusions of this article will be made available by the authors, without undue reservation.

## Author contributions

DF performed the experiments and wrote the draft. AF contributed to the conception and design of the study. All authors contributed to manuscript revision, read, and approved the submitted version.

## Funding

This work has been carried out with the financial support of Universidad Central del Ecuador.

## Conflict of interest

The authors declare that the research was conducted in the absence of any commercial or financial relationships that could be construed as a potential conflict of interest.

## Publisher's note

All claims expressed in this article are solely those of the authors and do not necessarily represent those of their affiliated organizations, or those of the publisher, the editors and the reviewers. Any product that may be evaluated in this article, or claim that may be made by its manufacturer, is not guaranteed or endorsed by the publisher.

## References

Buzuayehu, A., and Ananda, M. H. C. (2022). Insights into ZnO-based doped porous nanocrystal frameworks. *RSC Adv.* 12, 5816–5833. doi:10.1039/d1ra09152b

Chen, D., Cheng, Y., Zhou, N., Chen, P., Wang, Y., Li, K., et al. (2020). Photocatalytic degradation of organic pollutants using TiO2-based photocatalysts: A review. *J. Clean. Prod.* 268, 121725, doi:10.1016/j.jclepro.2020.121725

Deshmukh, S. P., Kale, D. P., Kar, S., Shirsath, S. R., Bhanvase, B. A., Saharan, V. K., et al. (2020). Ultrasound assisted preparation of rGO/TiO2 nanocomposite for effective photocatalytic degradation of methylene blue under sunlight. *Nano–Structures Nano-Objects* 21, 100407, doi:10.1016/j.nanoso.2019.100407

Flores-Oña, D., and Fullana, A. (2020). Carbon nanoparticles production using solvent assisted hydrothermal carbonization. *Diam. Relat. Mater.* 108, 107960, doi:10.1016/j.diamond.2020.107960

Hu, S., Tian, R., Wu, L., Zhao, Q., Jinlong, Y., Liu, J., et al. (2013). Chemical regulation of carbon quantum dots from synthesis to photocatalytic activity. *Chem. Asian J.* 8 (5), 1035–1041. doi:10.1002/asia.201300076

Kumar, A., and Pandey, G. (2017). A review on the factors affecting the photocatalytic degradation of hazardous materials. *Material Sci Eng Int J* 1 (3), 106–114. doi:10.15406/mseij.2017.01.00018

Lee, X., Hiew, B. Y. Z., Lai, Y. L., Gan, S., Thangalazhy-Gopakumar, S., and Rigby, S. (2019). Review on graphene and its derivatives: Synthesis methods and potential industrial implementation. *J. Taiwan Inst. Chem. Eng.* 98, 163–180. doi:10.1016/j.jtice.2018.10.028

Li, F., Qin, S., Jia, S., and Wang, G. (2021). Pyrolytic synthesis of organosilane-functionalized carbon nanoparticles for enhanced photocatalytic degradation of methylene blue under visible light irradiation. *Luminescence* 36 (3), 711–720. doi:10.1002/bio.3994

Li, F., Wang, G., Hongren, L., Li, Y., and Zhou, S. (2014). One-pot solvothermal synthesis of highly photoluminescent carbon nanoparticles and their photocatalytic application. *Mater. Lett.* 122 (21), 352–354. doi:10.1016/j.matlet.2014.01.095

Mahmud, R. A., Shafawi, A. N., Ali, K. A., Putri, L. K., Rosli, N. I. M., and Mohamed, A. R. (2020). Graphene nanoplatelets with low defect density as a synergetic adsorbent and electron sink for ZnO in the photocatalytic degradation of Methylene Blue under UV–vis irradiation. *Mater. Res. Bull.* 128, 110876, doi:10.1016/j.materresbull.2020.110876

Makuła, P., Pacia, M., and Macyk, W. (2018). How to correctly determine the band gap energy of modified semiconductor photocatalysts based on UV–Vis spectra. *J. Phys. Chem. Lett.* 9 (23), 6814–6817. doi:10.1021/acs.jpclett.8b02892

Mazrad, Z. A. I., Lee, K., Chae, A., In, I., Lee, H., and Park, S. Y. (2018). Progress in internally/externally-responsive fluorescent carbon nanoparticles for theranostic and sensing applications. *J. Mater. Chem. B* 6, 1149–1178. doi:10.1039/C7TB03323K

Miklos, D. B., Remy, C., Jekel, M., Linden, K. G., Drewes, J. E., and Hübner, U. (2018). Evaluation of advanced oxidation processes for water and wastewater treatment – a critical review. *Water Res.* 139, 118–131. doi:10.1016/j.watres.2018.03.042

Murugesan, A., Loganathan, M., Kumar, P. S., and Vo, D. N. (2021). Cobalt and nickel oxides supported activated carbon as an effective photocatalysts for the degradation Methylene Blue dye from aquatic environment. *Sustain. Chem. Pharm.* 21, 100406. doi:10.1016/j.scp.2021.100406

Rani, U. A., Ng, L. Y., Ng, C. Y., Mahmoudi, E., Ng, Y., and Mohammad, A. W. (2021). Sustainable production of nitrogen-doped carbon quantum dots for photocatalytic degradation of methylene blue and malachite green. *J. Water Process Eng.* 40, 101816, doi:10.1016/j.jwpe.2020.101816

Ranjith, K. S., Manivel, P., Rajendrakumar, R. T., and Uyar, T. (2017). Multifunctional ZnO nanorod-reduced graphene oxide hybrids nanocomposites for effective water

remediation: Effective sunlight driven degradation of organic dyes and rapid heavy metal adsorption. *Chem. Eng. J.* 325, 588–600. doi:10.1016/j.cej.2017.05.105

Román, S., Libra, J., Berge, N., Sabio, E., Ro, K., Li, L., et al. (2018). Hydrothermal carbonization: Modeling, final properties design and applications: A review. *Energies* 1 (1), 1–28. doi:10.3390/en11010216

Siddique, K., Rizwan, M., Shahid, M. J., Ali, S., Ahmad, R., and Rizvi, H. (2017). Textile wastewater treatment options: A critical review. *Enhancing Cleanup Environ. Pollut.* 2, 1–374. doi:10.1007/978-3-319-55423-5_6

Subagyo, R., Kusumawati, Y., and Widayatno, W. B. (2020). Kinetic study of methylene blue photocatalytic decolorization using zinc oxide under UV-LED irradiation. *AIP. Conf. Pro.* 2237 (1), 020001. doi:10.1063/5.0005263

Wang, D., Zhao, L., Ma, H., Zhang, H., and Guo, L. (2017). Quantitative analysis of reactive oxygen species photogenerated on metal oxide nanoparticles and their bacteria toxicity: The role of superoxide radicals. *Environ. Sci. Technol.* 51 (17), 10137–10145. doi:10.1021/acs.est.7b00473

Wang, H., Ye, Z., Liu, C., Li, J., Zhou, M., Guan, Q., et al. (2015). Visible light driven Ag/Ag3PO4/AC photocatalyst with highlyenhanced photodegradation of tetracycline antibiotics. *Appl. Surf. Sci.* 353, 391–399. doi:10.1016/j.apsusc.2015.06.125

Wang, L., Zhu, S., Wang, H., Qu, S., Zhang, Y., Zhang, J., et al. (2014). Common origin of green luminescence in carbon nanodots and graphene quantum dots. *American Chem. Soc.* 8 (3), 2541–2547. doi:10.1021/nn500368m

Yang, P., Zhao, J., Wang, J., Cui, H., Lai, L., and Zhu, Z. (2015). Pure carbon nanodots for excellent photocatalytic hydrogen generation. *RSC. Adv.* 5, 21332, doi:10.1039/c5ra01924a

Zhu, S., Meng, Q., Zhang, J., Song, Y., Zhang, K., Yang, B., et al. (2013). *Highly photoluminescent carbon dots for multicolor patterning, sensors, and bioimaging.* Changchun: National Science Foundation of China. doi:10.1002/ange.201300519

Zhuo, S., Shao, M., and Lee, S. (2012). Upconversion and downconversion fluorescent graphene quantum dots: Ultrasonic preparation and photocatalysis. *ACS Nano* 6 (2), 1059–1064. doi:10.1021/nn2040395